agriculture

MDPI

Article

The Inversion of Rice Leaf Pigment Content: Using the Absorption Spectrum to Optimize the Vegetation Index

Longfei Ma, Yuanjin Li, Ningge Yuan, Xiaojuan Liu, Yuyan Yan, Chaoran Zhang, Shenghui Fang and Yan Gong *

School of Remote Sensing and Information Engineering, Wuhan University, Wuhan 430072, China; longfei@whu.edu.cn (L.M.); liyuanjine@whu.edu.cn (Y.L.); yuanng@whu.edu.cn (N.Y.); xiaojliu@whu.edu.cn (X.L.); yanyuyan@whu.edu.cn (Y.Y.); rszcr16@whu.edu.cn (C.Z.); shfang@whu.edu.cn (S.F.)
* Correspondence: gongyan@whu.edu.cn

Abstract: The pigment content of rice leaves plays an important role in the growth and development of rice. The accurate and rapid assessment of the pigment content of leaves is of great significance for monitoring the growth status of rice. This study used the Analytical Spectra Device (ASD) FieldSpec 4 spectrometer to measure the leaf reflectance spectra of 4 rice varieties during the entire growth period under 4 nitrogen application rates and simultaneously measured the leaf pigment content. The leaf's absorption spectra were calculated based on the physical process of spectral transmission. An examination was conducted on the variations in pigment composition among distinct rice cultivars, alongside a thorough dissection of the interrelations and distinctions between leaf reflectance spectra and absorption spectra. Based on the vegetation index proposed by previous researchers in order to invert pigment content, the absorption spectrum was used to replace the original reflectance data to optimize the vegetation index. The results showed that the chlorophyll and carotenoid contents of different rice varieties showed regular changes during the whole growth period, and that the leaf absorption spectra of different rice varieties showed more obvious differences than reflectance spectra. After replacing the reflectance of pigment absorptivity-sensitive bands (400 nm, 550 nm, 680 nm, and red-edge bands) with absorptivities that would optimize the vegetation index, the correlation between the vegetation index, which combines absorptivity and reflectivity, and the chlorophyll and carotenoid contents of 4 rice varieties during the whole growth period was significantly improved. The model's validation results indicate that the pigment inversion model, based on the improved vegetation index using absorption spectra, outperforms the traditional vegetation index-based pigment inversion model. The results of this study demonstrate the potential application of absorption spectroscopy in the quantitative inversion of crop phenotypes.

Keywords: pigment content; absorption spectrum; reflection spectrum; vegetation index; rice

Citation: Ma, L.; Li, Y.; Yuan, N.; Liu, X.; Yan, Y.; Zhang, C.; Fang, S.; Gong, Y. The Inversion of Rice Leaf Pigment Content: Using the Absorption Spectrum to Optimize the Vegetation Index. *Agriculture* **2024**, *14*, 2265. https://doi.org/10.3390/agriculture14122265

Academic Editor: Kohei Koyama

Received: 26 October 2024
Revised: 29 November 2024
Accepted: 9 December 2024
Published: 11 December 2024

1. Introduction

Rice is one of the three major food crops in the world [1] Ensuring the safety of rice production is of great significance to world food security. In rice photosynthesis, the pigment content level is an important physiological indicator, which is closely related to the growth and development, photosynthetic capacity, nutrition, and environmental stress of rice [2,3]. Chlorophyll a and b and carotenoids are the main photosynthetic pigments, and their light absorption is in the visible region of the electromagnetic spectrum, ranging from 400 nm to 750 nm [4]. Chlorophylls play key roles in photosynthesis because of their light energy absorption and contribution to conversion into chemical energy [4]. Also, carotenoids perform physiological functions associated with photosynthesis, including a structural role in the organization of photosynthetic membranes. They also participate in light harvesting and energy transfer [5–7].

Traditional methods for the beam detection of pigment content, such as ultraviolet spectroscopy and fluorescence analysis, mainly rely on laboratory measurements. These methods require destructive sampling, which has the disadvantage of being time-consuming and

labor-intensive [8,9]. Spectroscopic technologies, the new tools for plant physiological and biochemical research, can reflect the growth status of plants through quantitative research on the reflectance of plant leaves [10,11]. For example, vegetation indices are used to assess the developmental responses of *Coleus* under different light qualities. Similarly, indices such as the Photochemical Reflectance Index (PRI) and the Modified Chlorophyll Absorption Ratio Index (MCARI) have demonstrated their effectiveness in characterizing the growth and developmental traits of *Viola* species under varying color temperatures [12,13]. Plant pigment content and spectral reflectance are closely related. The use of spectral data to invert pigment content is one of the current hot spots in plant phenotyping research [14,15]. Recently, the inversion of crop pigment content, using machine learning models and physical models based on the principle of radiative transfer principle, was reported. This involves a boosting regression algorithm [16] and the PROSPECT model [17]. However, current machine learning models and physical models each have their shortcomings [18,19]. The machine learning model has no interpretability in the data operation process [20] and cannot explain the biological mechanisms between the spectral information and the inversion parameters [21,22]. More importantly, the input of large amounts of training data is often required, which limits the application scenarios of machine learning models under certain conditions. As observation conditions such as time, place, and scale change, most models have to be retrained, which results in the poor transferability of machine learning models [23]. Physical models are based on biological and physical mechanisms, which are difficult to obtain directly. Also, there are great difficulties in the process of solving the physical model, which limits the further application space of physical models [24–26].

Retrieving leaf pigment content based on the empirical spectral vegetation index is the more robust and direct method of assessment [27]. The general idea of constructing a vegetation index is to combine two or more sensitive bands and one insensitive band of inversion indicators. Then, the bands can be normalized or ratio-processed to enhance the utilization rate of spectral information [28]. The reflectance spectrum is the common parameter used to construct a vegetation index in many studies. The leaf chlorophyll has a significant reflection effect in the green band and a significant absorption effect in the red and blue bands. The reflectivity of the near-infrared band has a significant effect on the ratio of the leaf mesophyll cell surface and the air space between cell relationships [29]. For example, the hyperspectral vegetation index was used in the inversion of the chlorophyll content of corn leaves and the results showed the best correlation between the Green Normalized Vegetation Index (GNDVI) and leaf chlorophyll content, yielding R^2 = 0.67 [30]. Meanwhile, a large number of vegetation indices have also been developed for the inversion of carotenoid content in leaves. Gitelson et al. [31,32] proposed the Carotenoid Concentration Index (CRI550, CRI700) and the modified carotenoid concentration index based on the near-infrared band (RNIR*CRI550, RNIR*CRI700). This showed that the bands of 515 nm, 550 nm, and 700 nm are sensitive to carotenoid content. Additionally, Hernández et al. [7] simplified the form of the Photochemical Reflectance Index (PRI) vegetation index and developed a modified Photochemical Reflectance Index (PRIm1) with values of 515 nm and 530 nm. Taken together, constructing a vegetation index based on the reflectance spectrum is beneficial to extracting physiological information about crops from spectral data. The use of a vegetation index to invert crop parameters has the advantages of being intuitive and interpretable [33,34].

However, most previous studies focusing on the reflectance spectra of leaves did not consider the relationship between plant leaves and the spectrum. The interaction between light and leaves includes reflection, absorption, and transmission. When a light beam impinges upon the leaf surface, a portion of it is directly reflected off the surface, while the transmitted light penetrates through the epidermis into the interior of the leaf, where it undergoes scattering. Within the leaf, the incident light is partially absorbed by the leaf's constituent materials. The process of light propagation within the leaf is notably influenced by both the circuitous path effect and the sieve effect, which significantly impact the leaf's net absorption capacity of light [35]. Consequently, the information

embedded within the absorption or transmission spectra of leaves can be harnessed for the monitoring of the physiological status of the foliage. Baranoski et al. [36] used the ratio of reflectance spectra and transmission spectra of maize leaves to detect water stress in maize leaves, demonstrating the application potential of transmission spectra and absorption spectra in the monitoring of crop growth conditions. Therefore, the mining of spectral information should not be limited to the reflection spectrum of leaves, as the absorption spectrum reflects the leaf structure, biochemical components, and other factors, also demonstrating the role of stable light sources to a certain extent [37]. Studying the absorption spectra of leaves is more conducive to exploring the biological mechanisms that exist between spectra and leaf physiological and biochemical components. However, only stochastic leaf radiation models (LMFOD1), Leaf Incorporating Biochemistry Exhibiting Reflectance and Transmittance Yields (LIBERTY) models, and the stochastic model for leaf optical properties (SLOP) can determine the absorption spectrum in the visible range of a single pigment [38]. The LIBERTY model is specially designed for pine needles and does not apply to all plant leaves. The SLOP model is an improved version of the LFMOD1 model; the SLOP model simulates the transmission process of light inside the leaves based on the Markov chain principle. However, the SLOP model poses practical challenges, as it necessitates the establishment of detailed leaf structural parameters that are typically hard to accurately specify in applications [39–41]. Therefore, in this study, we have optimized the methodologies used for measuring and calculating leaf absorption spectra, reducing the number of parameters required in the process. Additionally, the absorption spectra derived from our research were utilized to refine conventional vegetation indices, with an investigation into the efficacy of these optimized indices in the inversion of leaf pigment content.

In summary, the objectives of this study were to (i) observe the changes in chlorophyll levels and carotenoids in different varieties of rice under different nitrogen application rates during the whole growth period, (ii) to clarify the superior accuracy of the absorption spectrum compared to the reflection spectrum at different pigment contents in rice leaves by calculating the absorption spectrum and transmission spectrum of fresh leaves, and (iii) to indicate the potential of vegetation indices, as improved by employing absorption spectra, in estimating the pigment contents of rice leaf samples.

2. Materials and Methods

2.1. Field Experiment Design

The experimental was carried out in 2023 in a field which is located at the Rice Planting Base of Wuhan University, Huashan, Wuhan City, Hubei Province (114.52 E, 30.55 N). The schematic diagram of the field experiment is shown in Figure 1. The area is located in a humid subtropical monsoon climate zone, with an average annual rainfall of 1269 mm and an average annual temperature of 15.8–17.5 °C. Four different rice varieties were selected for this experiment, including two japonica rice varieties—Chang jing you 582 and Zhong hua 11—and two indica rice varieties, namely, Feng liang you 4 and Luo you 9348. We set 4 different nitrogen fertilizer application rates for each rice variety: 0 kg/ha (0 N), 35.1 kg/ha (1/4 N), 140.4 kg/ha (1 N), and 280.8 kg/ha (2 N). The dosage of phosphate fertilizer and potassium fertilizer remained the same, with a total of $4 \times 4 = 16$ treatments performed. Each treatment was repeated three times, for a total of $16 \times 3 = 48$ plots. Each plot's area was 4 m × 5 m = 20 m^2. The rice was transplanted on 25 June 2023. We applied nitrogen fertilizer twice after transplanting. The two application amounts of nitrogen fertilizer were 60% and 40% of the total amount, respectively. The field soil samples were collected before transplanting, and the basic fertility of the field soil was measured. The measurement results are shown in Table 1. The rest of the field management practices are consistent with conventional local management measures.

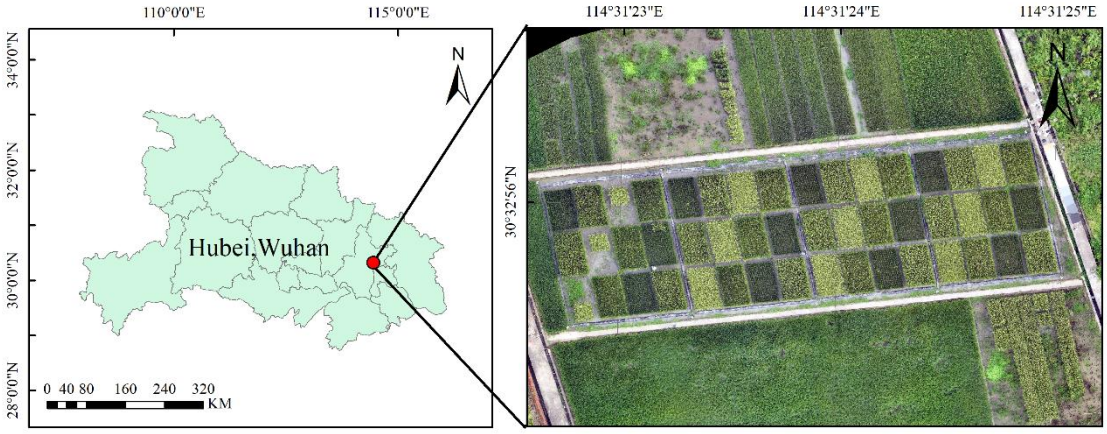

Figure 1. The field experiment area and a map of its location in Wuhan, Hubei. The (**left**) figure illustrates the location map of Wuhan City in Hubei province, and the (**right**) diagram depicts the field experiment's layout.

Table 1. The basic fertility status of the experimental field soil.

Measurement Indicators	Alkaline Hydrolysis of Nitrogen (mg/kg)	Total Nitrogen (mg/kg)	Available Phosphorus (mg/kg)	Available Potassium (mg/kg)
Contents	190.075	1470.5	139.5	46.8

2.2. Spectral Data and Measured Data Collection

After 30 days of transplanting, samples were taken every 10 days for each plot. During sampling, three plants that could represent the growth status of the entire plot were selected. The roots were dug back and cleaned for further processing in the laboratory. We selected the last expanded leaf of the sample plant and used ASD FieldSpec 4 to collect the spectral data. We used the leaf clip to measure the reflectance spectrum (Figure 2a). The leaf clip of the instrument came with a stable halogen light source. The ASD FieldSpec 4 host can obtain spectral reflectance in the range of 350–2500 nm. The spectral resolution of 350–1400 nm is 3 nm and between 1400 and 2500 nm the spectral resolution is 5 nm. The leaf clip is divided into a black panel and a white panel. After using the white panel for spectral correction, the rice leaf reflectance spectrum is measured using the black panel and the white panel as the background, respectively. The measurement is repeated three times for each plant, and the reflection spectrum is collected five times for each measurement; the five spectral curves are averaged as the leaf reflectance spectral curve of each plot. After the spectrum measurement is completed, it is necessary to use a leaf punch with a diameter of 6 mm to drill holes and sample the same positions on the leaves. The weight (W) of each circular leaf extract was weighed using an analytical balance, and the circular leaf sample was chopped and placed in a dark place with 10 mL 95% ethanol for static extraction for 24 h. The absorbance of the extracted solution was measured at wavelengths of 470 nm, 646 nm, and 663 nm with a spectrophotometer, and the light absorption value optical density (OD) of the sample was recorded at the three bands, respectively. The contents of chlorophyll a (Chla), chlorophyll b (Chlb), and carotenoid (Car) were calculated according to the scheme proposed by Lichtenthaler [42]. The pigment content unit employed when using this method was mg/g. In this experiment, the circular leaf area measured by the perforator in the sampling process can be calculated. As such, the leaf pigment content mg/g is converted to mg/cm^2 for subsequent analysis.

$$\text{Chla (mg/L)} = 12.21*OD_{663} - 2.81*OD_{646}$$

$$\text{Chlb (mg/L)} = 20.13*OD_{646} - 5.03*OD_{663}$$

$$\text{Chla + b (mg/L)} = \text{Chla (mg/L)} + \text{Chlb (mg/L)}$$

$$\text{Car (mg/L)} = (1000*\text{OD}_{470} - 3.27*\text{Chla} - 104*\text{Chlb})/229$$

$$\text{Pigment (mg/g)} = \frac{C(\text{mg/L}) * 10\text{mL}}{W(\text{g}) * 1000}$$

$$\text{Pigment content (mg/cm}^2) = \frac{pigment(\text{mg/g}) * W(\text{g})}{\pi r^2}$$

where the OD is the optical density at each band, W is the weight of the leaf sample, and the * represents the multiplication sign.

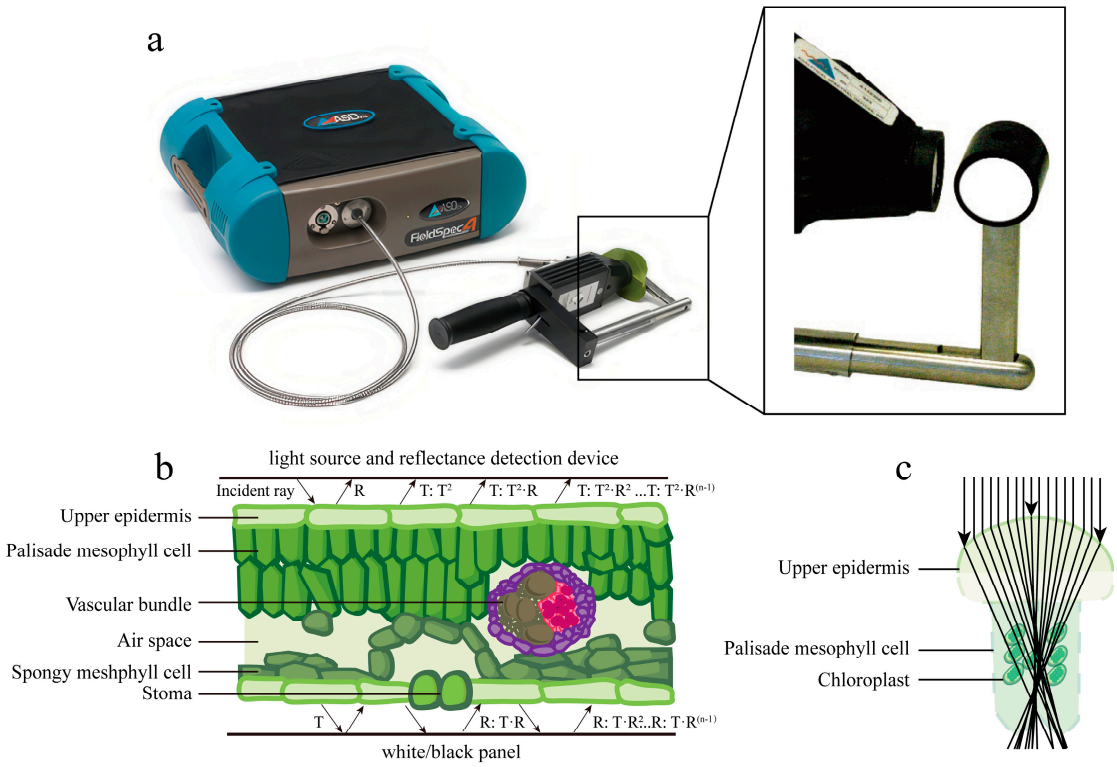

Figure 2. (**a**) The ASD host and leaf clip for the determination of leaf spectra; (**b**) schematic diagram of the interaction between light and leaves during spectrometry; (**c**) schematic diagram of the aggregation effect of leaf epidermal cells on light.

2.3. Modeling Theory

The schematic diagram of the leaf structure for most leaves whose upper surfaces receive light is shown in Figure 2b. For the reflectance spectrum, when light is irradiated on the leaves of the upper surface, the villi and the waxy layer of the upper epidermis of the leaf have a significant impact on the light reflection. The surface villi enhance the reflectivity throughout the visible light region, but the effect is variable in the near-infrared region. The waxy layer increases the surface reflectivity throughout the visible and near-infrared regions; this effect is due to the Rayleigh scattering effect, and the effect is more obvious at short wavelengths [43]. For the absorption spectrum, when light passes through the upper epidermis of the leaf and enters the inside of the leaf, both the palisade tissue and the sponge in the leaf absorb light. Chloroplasts in palisade tissues are mainly related to chlorophyll absorption bands, while spongy tissues mainly absorb weak absorption bands [44]. At the same time, we took into account the shape characteristics of the epidermal cells on the leaves. The upper epidermal cells of plants have the characteristics of protrusions (Figure 2c). The structures of these protrusions have the effect of gathering light, meaning that more light will enter the vegetation and enhance the absorption effect of light on the

leaves [45]. Therefore, chlorophyll absorption bands are selected as the construction scheme of the new vegetation index according to this feature.

The gap between the absorption spectrum and reflection spectrum is enhanced to solve the saturation effect of the vegetation index. Observing the curves of the absorption spectra and reflection spectra, shown in Figure 3, it can be seen that in the chlorophyll absorption-sensitive band region, at 490 nm, 550 nm, and 700 nm, the difference between the absorption spectra of pigment content in the leaves of different varieties was significantly higher than the same difference in terms of the reflection spectra at the corresponding band. Therefore, when constructing the vegetation index combined with the absorption spectrum, the reflection spectrum of the pigment absorption-sensitive band is replaced by the absorption spectrum, which will further amplify the difference between spectra and optimize the inversion effect of the vegetation index based on this principle. In this study, the vegetation index we selected is shown in Table 2.

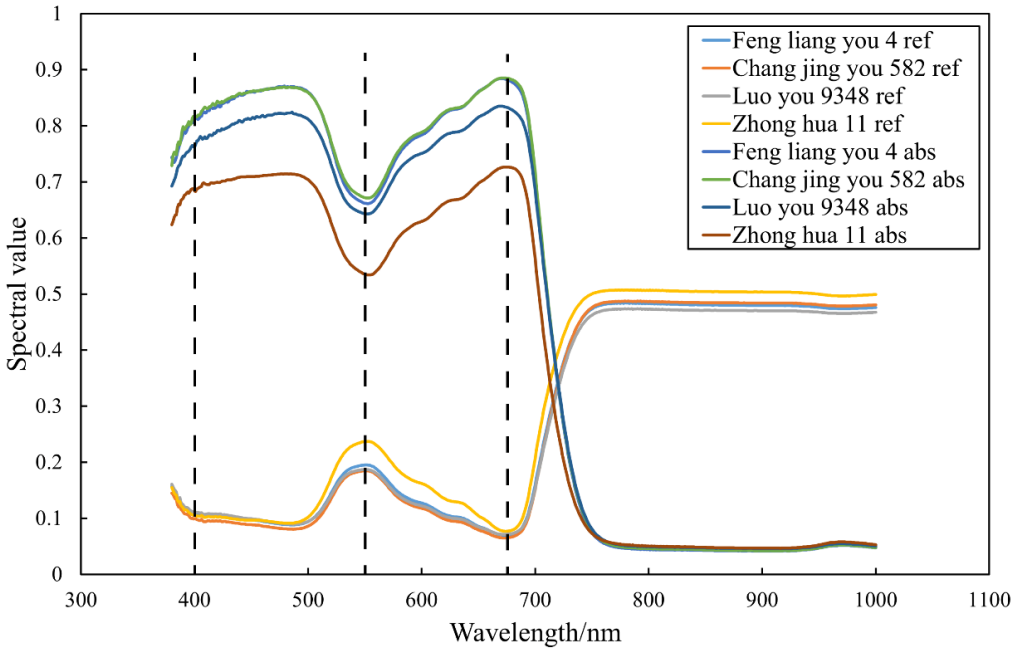

Figure 3. Absorption spectra and reflectance spectra of four varieties of rice under 1 N conditions at 101 days after transplanting (where ref represents reflectance spectra and abs represents absorption spectra).

Table 2. The vegetation indices employed in this study. * represents the multiplication sign.

	Name	Formula	Reference
Chlorophyll	Leaf chlorophyll index (LCI)	$\frac{850\ \text{nm}-710\ \text{nm}}{850\ \text{nm}+680\ \text{nm}}$	[46]
	Chlorophyll index green (CIgreen)	$\frac{850\ \text{nm}}{550\ \text{nm}}-1$	[31,47]
Normalization	Normalized difference (ND)	$\frac{\lambda_1-\lambda_2}{\lambda_1+\lambda_2}$	[48]
Ratio	Simple ratio	$\frac{\lambda_1}{\lambda_2}$	[49]
Cartonides	CRI 550	$\frac{1}{515\ \text{nm}}-\frac{1}{550\ \text{nm}}$	[31]
	CRI 700	$\frac{1}{515\ \text{nm}}-\frac{1}{700\ \text{nm}}$	[31,32]
	RNIR*CRI550	$\left(\frac{1}{515\ \text{nm}}-\frac{1}{550\ \text{nm}}\right)*770\ \text{nm}$	[31,32]
	RNIR*CRI700	$\left(\frac{1}{515\ \text{nm}}-\frac{1}{550\ \text{nm}}\right)*770\ \text{nm}$	[31,32]
	PRIm1	$\frac{515\ \text{nm}-530\ \text{nm}}{515\ \text{nm}+530\ \text{nm}}$	[7]

2.4. Spectral Processing and Model Selection and Evaluation

Existing leaf optical transfer models, such as the PROSPECT model, are developed based on the plate model, which considers the incident angle of the light, the number of internal layers of non-compact leaves, and the transmission and refraction coefficients between various materials. The reflectance and transmittance of the leaf are simulated through these parameters [50]. In this study, the leaf is directly regarded as a translucent whole. The attenuation law of light during the transmission process is directly considered, but the physics of light inside the leaf is not considered. In the change process, the transmission spectra and absorption spectra of the leaves are calculated from the known reflection spectra measured on the blackboard and whiteboard of the ASD spectrometer. The reflectance of the whiteboard of the spectrometer is considered to be 1 in each band, and the blackboard reflectance is 0 in each band. The black background plate and the white background plate are used to measure the leaf reflectivity—ρBlack (ρB) and ρWhite (ρW), respectively—in order to calculate the leaf transmittance (T_L). Figure 2b shows a schematic diagram of the interaction between light and leaves during spectrum measurement.

When the lower reflector is a whiteboard, the leaf clip emits light and shines on the leaf. The first reflected light is r, and the transmitted light is T. The transmitted light is reflected by the whiteboard and penetrates the leaf. The remaining light is T^2. It is necessary to consider that the light passes through infinite reflection and transmission (Figure 2b):

$$\rho_{\mathrm{W}} = r(\lambda) + T(\lambda)^2 + T(\lambda)^2 r(\lambda) + \ldots + T(\lambda)^2 r(\lambda)^{n-1}$$

When $n = +\infty$,

$$\rho_W = r(\lambda) + T(\lambda)^2 \left(\frac{1}{1 - r(\lambda)} \right)$$

For any wavelength, there is

$$T_L = \sqrt{(\rho_W - \rho_B) * (1 - \rho_B)}$$

Therefore

$$A = 1 - \rho_B - T_L$$

where A represents the absorption spectra, ρ_W, and ρ_B represent the leaf reflectance measured with the whiteboard and blackboard as the base, respectively, and T_L is the leaf transmittance.

Optimizing a vegetation index based on leaf reflectance and leaf absorptivity, we examined the correlation between different vegetation indices and pigment content based on a linear regression model. The models were validated using the leave-one-out cross-validation method, employing using coefficient of determination (R^2) and root-mean-square error (RMSE) to evaluate the performance of the models. Figure 1 was drawn using ArcGIS (https://www.esri.com/en-us/arcgis/geospatial-platform/overview), Figure 2 was drawn using Adobe Illustrate (https://www.adobe.com/hk_en/products/illustrator.html), and Figures 3–9 were drawn using ggplot2 package (https://CRAN.R-project.org/package=ggplot2) in Rstudio platform (version: 2023.12.0), the calculation formulas of R^2 and RMSE are as follows:

$$R^2 = 1 - \frac{\sum (y - \hat{y})^2}{\sum (y - \overline{y})^2}$$

$$RMSE = \sqrt{\frac{1}{n} \sum_{i=1}^{n} (y_i - \hat{y})^2}$$

After reviewing the literature, the pigment-sensitive band was selected. In this experiment, based on previous research advancements [51] and considerations for the extension of future work, five bands, 490 nm, 515 nm, 530 nm, 550 nm, 700 nm, and 770 nm, were selected as the pigment-sensitive bands. The absorption and reflectivity values of the above

bands were used to optimize the vegetation index. The selected bands were normalized and ratioed according to the typical vegetation index calculation mode. At the same time, the typical vegetation indices, namely, leaf chlorophyll index (LCI) and chlorophyll index green (CIgreen), are commonly used to invert the leaf chlorophyll content. The typical vegetation indices of CRI550, CRI700, RNIR*CRI550, RNIR*CRI700, and PRIm1, which are commonly used to invert carotenoid content, were selected. The optimized vegetation index was constructed using the reflection spectrum, the absorption spectrum, and the reflection spectrum combined with the absorption spectrum, respectively. The reflection spectrum was marked as λ_{ref}, and the absorption spectrum was marked as λ_{abs}. We analyzed the effect of the vegetation index constructed by different combinations of spectra in terms of retrieving rice leaf pigments.

3. Result

3.1. Analysis of Pigment Content in Leaves of Different Rice Varieties Throughout the Growth Period

Figure 4 shows the changing trend in the chlorophyll content of the four varieties used in the experiment at different dates after transplanting. From the perspective of the whole growth period, the chlorophyll content of the four varieties showed a trend of first increasing and then decreasing. For the Chang jing you 582 variety, the chlorophyll content in the leaves showed a slowly increasing trend from 51 days to 70 days after transplanting. Then, from 79 days to 120 days after transplanting, the chlorophyll content in the leaves showed a slowly decreasing trend. For the Feng liang you 4 variety, the chlorophyll content of leaves increased during the entire growth period and then declined rapidly. The chlorophyll content of the Luo you 9348 variety under four nitrogen treatments remained unchanged from 51 days to 101 days after transplanting, while the pigment content under four nitrogen treatments showed a rapid decline from 111 days to 120 days after transplanting. The chlorophyll content of the Zhong hua 11 variety showed a similar change trend during the whole growth period, as did that of Feng liang you 4. The chlorophyll content gradually increased from day 51 to day 70 after transplanting and gradually decreased under all nitrogen treatments after being transplanted at day 70.

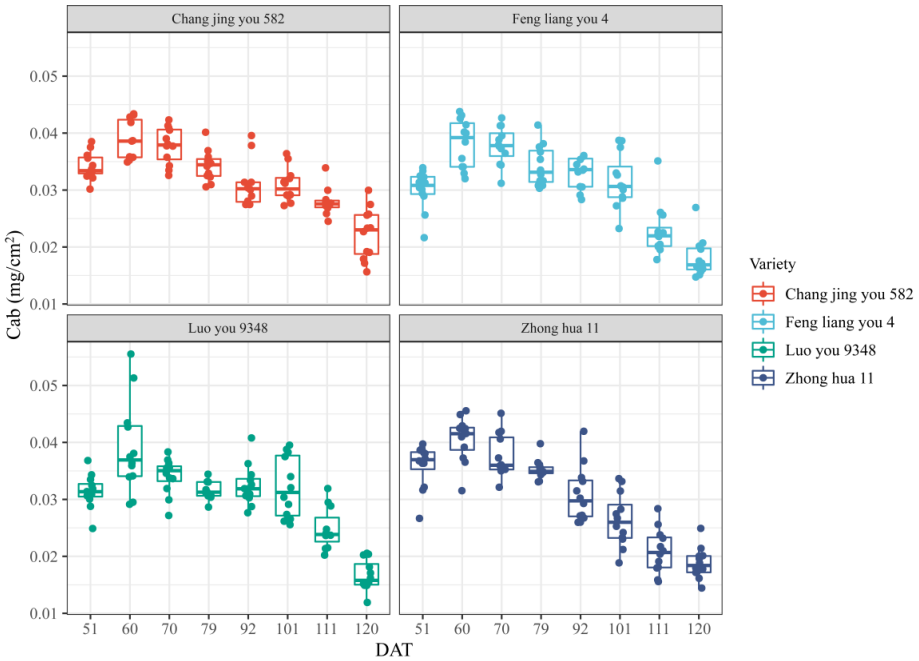

Figure 4. Change trends in the chlorophyll content in the leaves of four rice varieties throughout the growth period (four rice varieties: Chang jing you 582 (red), Feng liang you 4 (blue), Luo you 9348 (green), Zhong hua 11 (purple)). DAT represents days after transplanting; unit: days. Cab represents the total content of chlorophyll a and chlorophyll b; unit: mg/cm^2.

Figure 5 shows the changing trend of carotenoid content in the leaves of 4 varieties in the whole growth period. The carotenoid content of the Chang jing you 582 variety showed a gradually decreasing trend from 51 days to 92 days after transplanting, and significantly increased on 101 days after transplanting. While the carotenoid content of Chang jing you 582 decreased to a low level and remained the same from 111 days to 120 days after transplanting, the carotenoid content in the leaves of Feng liang you 4 showed a slowly decreasing trend from 51 to 101 days after transplanting and then decreased rapidly at 111 and 120 days after transplanting. The changing trend in the carotenoid content of the Luo you 9348 variety during the whole growth period was similar to that of Chang jing you 582. During the whole growth period, the carotenoid content in leaves showed a slow decrease. However, it then increased and dropped to a lower level. The carotenoid content of Zhong hua 11 showed a rapid decline from 51 days to 70 days after transplanting, remained unchanged from 70 days to 101 days after transplanting, and rapidly decreased to a low level at 111 days and 120 days after transplanting.

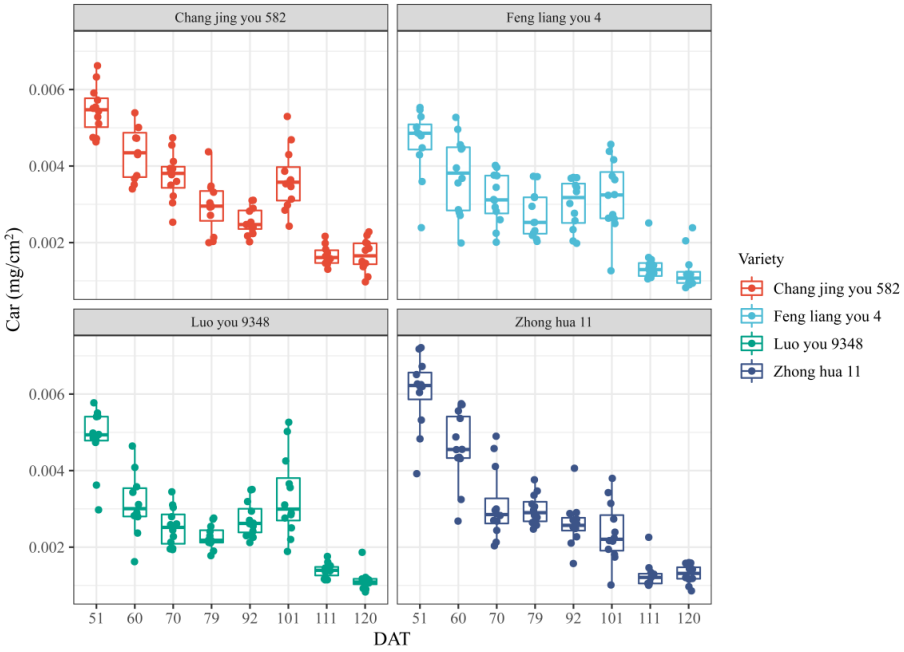

Figure 5. Change trends in the carotenoid content in leaves of four rice varieties throughout the growth period (four rice varieties: Chang jing you 582 (red); Feng liang you 4 (blue); Luo you 9348 (green); Zhong hua 11 (purple)). DAT represents days after transplanting; unit: days. Car represents the content of carotenoids, unit: mg/cm^2.

3.2. Correlation Analysis Between Chlorophyll Content and Vegetation Index

A correlation analysis was conducted on the chlorophyll content of the four varieties observed throughout the growth period. The results (Figure 6a) show that the correlation between the traditional vegetation index LCI, calculated based on reflectance, and CIgreen and chlorophyll content was good for the four varieties examined in this experiment. Among the vegetation indexes used in this study, the highest correlation with chlorophyll content was seen for the ratio vegetation index. For this, the correlation R^2 between the chlorophyll content of Zhong hua 11 and $700_{abs}/490_{ref}$ reached 0.761. Based on the normalized vegetation index and simple ratio vegetation index at 700 nm and 490 nm, the vegetation index calculated using absorbance has a higher correlation with pigment content than the vegetation index calculated based on reflectance. The correlation analysis between the simple ratio vegetation index and chlorophyll content shows that the vegetation index that uses both absorptivity and reflectance is more effective. As for the vegetation index developed for the inversion of carotenoid content, $CRI550_{ref}$ also showed

good correlation with chlorophyll content. However, using the original calculation method to replace reflectance with absorbance, the correlation between the two decreased. We further combined the absorbance and reflectance, and used the reflectance at 515 nm and the absorbance at 550 nm to calculate the correlation between the CRI $515_{ref} - 550_{abs}$ index and the chlorophyll content. Compared with CRI 700_{ref}, CRI 700_{abs}, and CRI $515_{ref} - 700_{abs}$, the R^2 of CRI $515_{ref} - 700_{abs}$ was the highest. Compared with RNIR*CRI 700_{ref}, PRIm1, and the corresponding calculated vegetation index, the correlation of the vegetation index calculated by absorption rate was better overall.

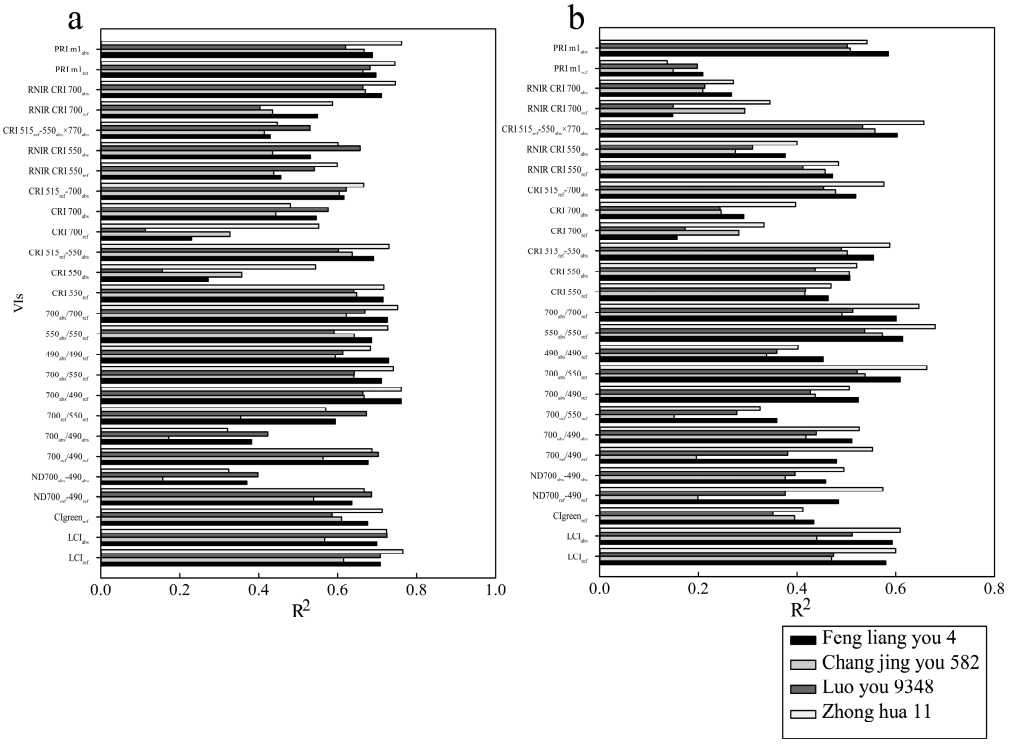

Figure 6. The correlation between pigment contents in leaves of four rice species and vegetation indexes (VIs): (**a**) the total content of chlorophyll a and chlorophyll b with vegetation indexes; (**b**) carotenoid contents with vegetation indexes. The picture shows the determination coefficient of the correlation between the pigment content of four rice varieties and each vegetation index. For Feng liang you 4 varieties, $700_{abs}/490_{ref}$ has the highest correlation with chlorophyll content, and CRI $515_{ref} - 550_{abs} \times 770_{ref}$ has the highest correlation with carotenoid content. For Chang jing you 582 varieties, $700_{abs}/490_{ref}$ has the highest correlation with chlorophyll content, and $550_{abs}/550_{ref}$ has the highest correlation with carotenoid content. For Luo you 9348 varieties, LCI_{abs} has the highest correlation with chlorophyll content, and CRI $515_{ref} - 550_{abs} \times 770_{ref}$ has the highest correlation with carotenoid content. For Zhong hua 11 varieties, LCI_{ref} has the highest correlation with chlorophyll content, and $550_{abs}/550_{ref}$ has the highest correlation with carotenoid content.

3.3. Correlation Analysis Between Carotenoid Content and Vegetation Index

As can be seen from Figure 6b, using the traditional vegetation index developed for chlorophyll, LCI calculated based on absorption rate had a better correlation with Feng liang you 4, Luo you 9348, and Zhong hua 11. Compared with the vegetation index calculated via normalized calculation, the R^2 values of varieties except Chang jing you 582 improved significantly. There was no significant difference in the determining coefficient R^2 between the carotenoid content and vegetation index of the other three varieties. Compared with the ratio-type vegetation index, the vegetation index calculated using the absorption rate had a good correlation with carotenoids, and the R^2 value of Zhong hua 11 and $550_{abs}/550_{ref}$ was the highest, reaching 0.68. For the vegetation index developed by the inversion of carotenoids, CRI550, CRI700, and CRI$515_{ref} - 550_{abs} \times 770_{abs}$ showed the best

correlations with the carotenoid content of the four kinds of rice, combining absorptivity and reflectivity. The determination coefficients of PRIm1 and carotenoids, determined based on the absorption rate, were higher than those of $PRIm1_{ref}$.

3.4. Model Validation and Accuracy Evaluation

In this study, we first selected the vegetation index with the highest R^2, corresponding to chlorophyll and carotenoids, for each variety based on the work shown in Figure 6. We found that the chlorophyll content of Zhong hua 11 variety had the highest correlation with the LCI (Figure 7m), while the rest had the highest correlation with the absorption spectrum vegetation index. Therefore, we selected the corresponding reflectance spectrum vegetation index and absorption spectrum vegetation index to construct the pigment content inversion model and we verified its accuracy. The results are shown in Figures 7 and 8. Figure 8 shows the verification effect of the pigment content inversion model based on the reflectance spectrum vegetation index of four rice varieties, and Figure 7 shows a scatter plot of the vegetation index with the highest correlation and the pigment content, indicating the verification effect of the pigment content inversion model based on the absorption spectrum vegetation index. A comparison of Figures 7 and 8 reveals that, among the tested varieties, only Zhong hua 11 (Figures 7n and 8g) exhibited higher validation accuracy for chlorophyll estimation using vegetation indices derived from reflectance spectra compared to those based on absorption spectra. For the remaining varieties, the validation accuracy of models based on absorption spectrum vegetation indices was superior, being characterized by higher R^2 values and lower RMSE values.

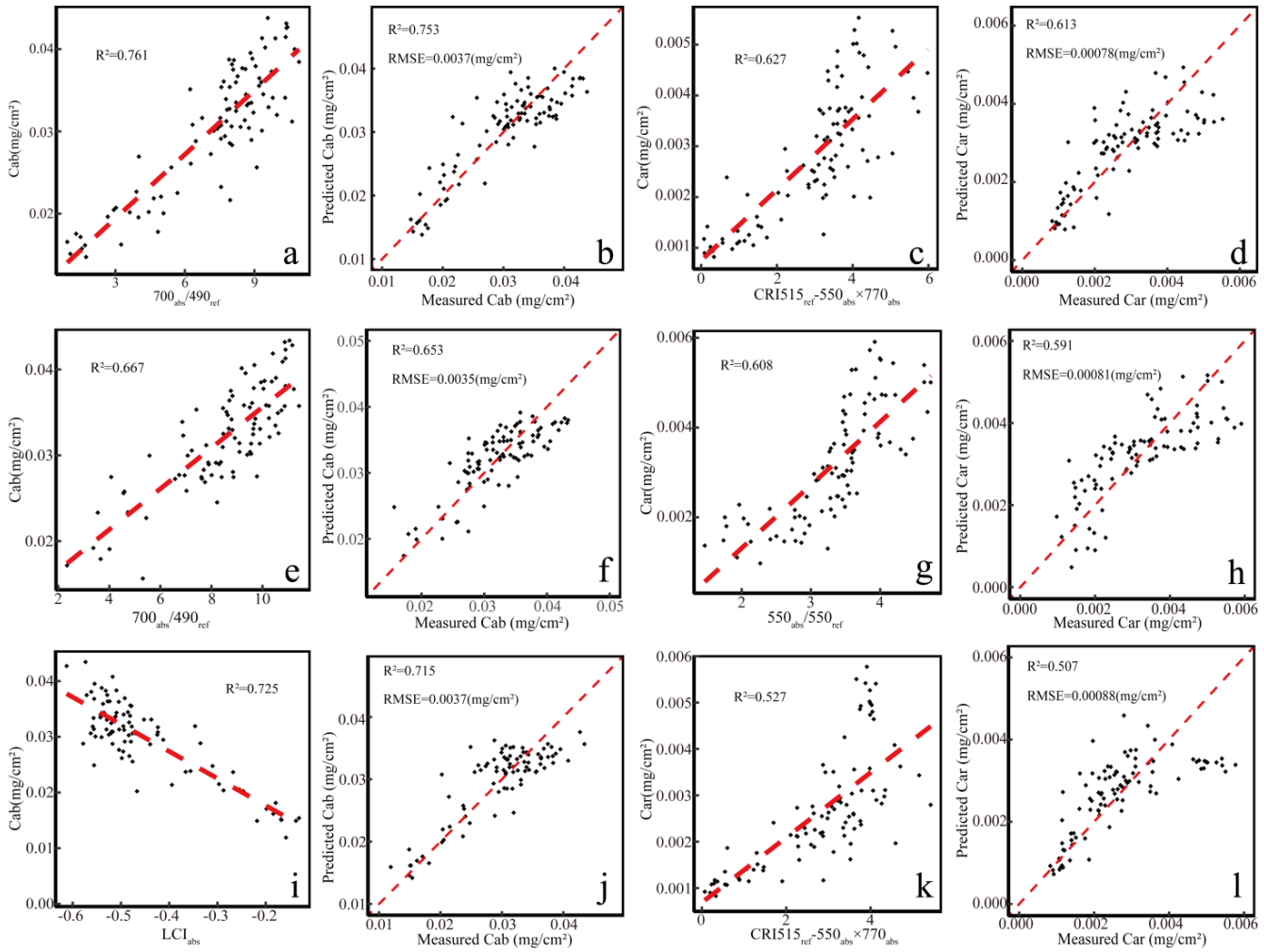

Figure 7. *Cont.*

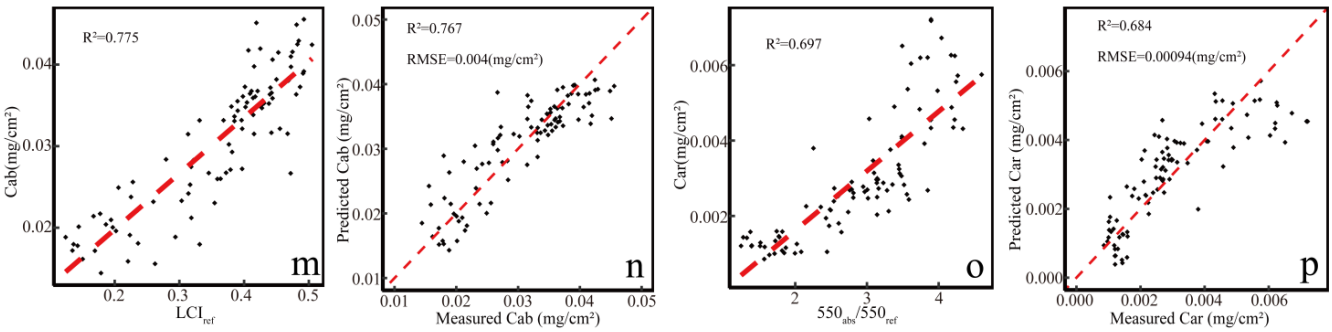

Figure 7. Correlation scatter plots of selected vegetation indexes, pigment contents, and model verification accuracies. Feng liang you 4 variety: (**a**) Correlation diagram between chlorophyll content and $700_{abs}/490_{ref}$. (**b**) Verification results of chlorophyll content inversion model. (**c**) Correlation diagram between carotenoid content and $CRI515_{ref} - 550_{abs} \times 770_{ref}$. (**d**) Verification results of carotenoid content inversion model. Chang jing you 582 varietI(**e**) Correlation diagram between chlorophyll content and $700_{abs}/490_{ref}$. (**f**) Verification results of chlorophyll content inversion model. (**g**) Correlation diagram between carotenoid content and $550_{abs}/550_{ref}$. (**h**) Verification results of carotenoid content inversion model. Luo you 9348 variety: (**i**) Correlation diagram between chlorophyll content and LCI_{abs}. (**j**) Verification results of chlorophyll content inversion model. (**k**) Correlation diagram between carotenoid content and $CRI515_{ref} - 550_{abs} \times 770_{abs}$. (**l**) Verification results of carotenoid content inversion model. Zhong hua 11 variety: (**m**) Correlation diagram between chlorophyll content and LCI_{ref}. (**n**) Verification results of chlorophyll content inversion model. (**o**) Correlation diagram between carotenoid content and $550_{abs}/550_{ref}$. (**p**) Verification results of carotenoid content inversion model.

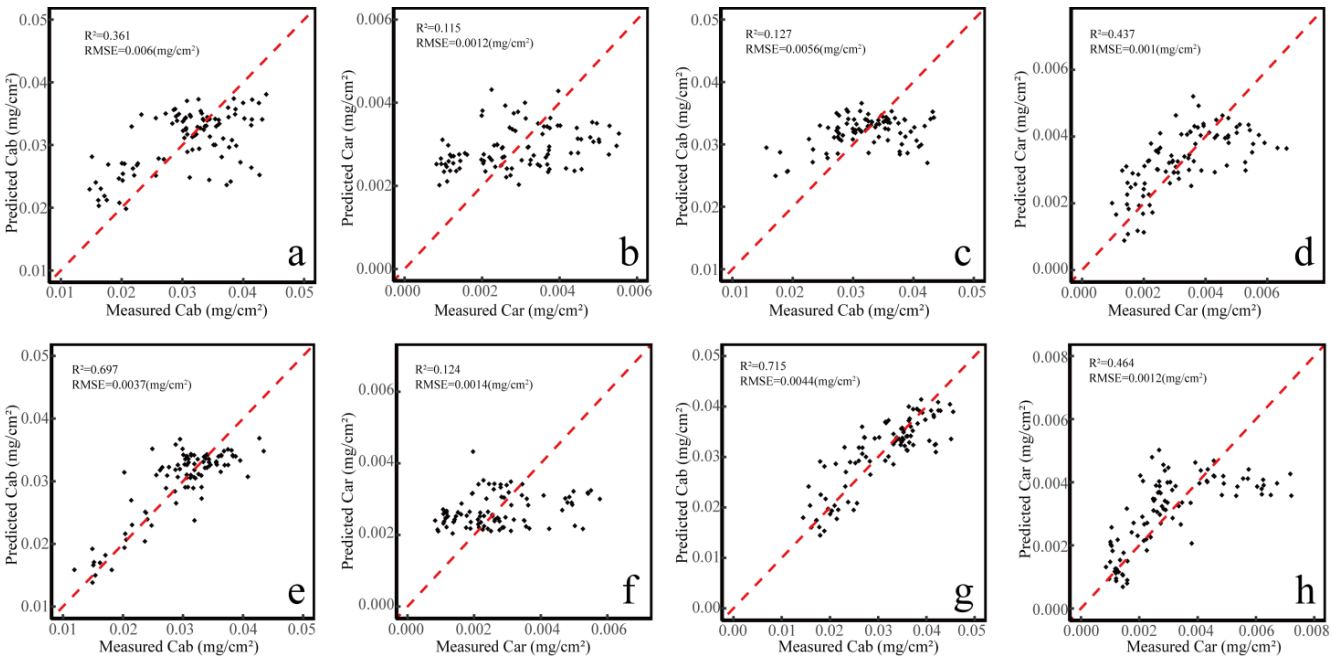

Figure 8. The accuracy validation of pigment content inversion models based on traditional reflectance spectroscopy vegetation indices. Feng liang you 4: (**a**) The accuracy validation of the chlorophyll content inversion model. (**b**) The accuracy validation of the carotenoid content inversion model. Chang jing you 582: (**c**) The accuracy validation of the chlorophyll content inversion model. (**d**) The accuracy validation of the carotenoid content inversion model. Luo you 9348: I The accuracy validation of the chlorophyll content inversion model. (**f**) The accuracy validation of the carotenoid content inversion model. Zhong hua 11: (**g**) The accuracy validation of the chlorophyll content inversion model. (**h**) The accuracy validation of the carotenoid content inversion model.

4. Discussion

The rice varieties used in this study were two indica rice (Feng liang you 4 and Luo you 9348) and two japonica rice (Chang jing you 582 and Zhong hua 11). Generally speaking, under the same conditions, the leaf color of japonica rice was a darker green than that of indica rice [52]. Therefore, we focused on the differences between different rice varieties and introduced the vegetation index of the absorption spectrum to the pigment inversion potential of different rice varieties. We will now discuss the characteristics of the variety itself, the spectral characteristics, and the performance ability of the vegetation index with the introduction of the absorption spectrum.

4.1. Change Characteristics of Pigment Content During the Whole Growth Period of Indica Rice and Japonica Rice

During the growth of rice, chlorophyll is an important photosynthetic substance. The differences in the changing trend in chlorophyll content between japonica rice and indica rice during development indicate that there are differences in the period of the accumulation of photosynthetic products between japonica rice and indica rice. Gong et al. [53] showed that indica rice had faster dry matter accumulation and a faster population growth rate in the early growth period (before the jointing stage), and faster senescence in the later growth period (maturity stage). The changing trend in chlorophyll content in indica and japonica rice displayed in this study was consistent with the above conclusions.

Carotenoids play an important role in the growth and development of higher plants. They participate in the process of light energy absorption in plants. Carotenoids absorb light energy in blue-green areas and expand the range of photon capture in plants [54]. At the same time, carotenoids transfer energy to chlorophyll, enhancing the photosynthesis of the thylakoids [55]. Carotenoids also protect chlorophyll molecules from reactive oxygen species [56]. Some 101 days after transplanting (late August and early September), the light intensity in the experimental area was very high. At the same time, most of the rice in the field was in the filling and milky stages. At this time, the photosynthesis of rice leaves was enhanced to accumulate more dry matter in order to promote yield formation, and so more carotenoids were needed to remove the free radicals produced by the leaves during photosynthesis and to protect the leaves [57]. Therefore, the carotenoid content of rice showed a brief increase 101 days after transplanting (Figure 5). In the study, leaf carotenoid content of indica and japonica rice showed a gradual decline during the whole growth period and a rapid decline in the later growth period, proving that indica and japonica rice have the same characteristics in terms of aging. Rottet et al. [58] showed that, with leaf aging and seed maturation, carotenoids undergo programmed degradation. This conclusion is consistent with the trend presented by the data in this study.

4.2. Difference Analysis of Spectral Reflectance and Absorptivity of Leaves

Figure 3 shows the spectral curves of the reflectance and absorptivity of 4 rice varieties under 1 N treatment 101 days after transplanting. Figure 9 shows the distribution of the reflectance spectral curve and absorption spectral curve of the Zhong hua 11 variety during the whole growth period under 1 N treatment. The range of 400 nm to 700 nm is the main band of pigment absorption, and the concentration of photosynthetic pigment molecules largely determines the light absorption rate of leaves [59]. In Figure 3, the reflectance curves of the four varieties showed no obvious difference, while the corresponding absorption spectra showed obvious differences, which proved that the absorption spectra could show more details than the reflected spectra [60]. The leaf pigment content of Zhong hua 11 was slightly lower than that of the other three varieties 101 days after transplanting (Figures 4 and 5), and the reflectance spectrum of Zhong hua 11 in the same period was slightly higher than that of the other three varieties, standing near 520 nm (Figure 3). The corresponding absorption spectra show obvious differences at 400–700 nm, indicating that the absorption spectra are more sensitive to the pigment content. Cavender et al. [61] pointed out that the light reflection of the epidermal cells of leaves carries

less information inside the leaves, and so the absorption spectrum has more correlation with information such as material content and the structure inside the leaves. Figure 9 shows that the reflectance and absorptivity have opposite change trends at 400–700 nm, but from the perspective of spectral change range, the absorptivity curve shows a more obvious difference than the reflectance curve. Therefore, when the relationship between pigment content and spectrum is established, the absorption spectrum shows a greater difference than the reflected spectrum in the process of constructing the vegetation index, and the mathematical operation of constructing the vegetation index can further amplify this gap [62]. This feature of the absorption spectrum can alleviate the saturation effect of the traditional vegetation index and improve the accuracy and adaptation range of the pigment content estimation.

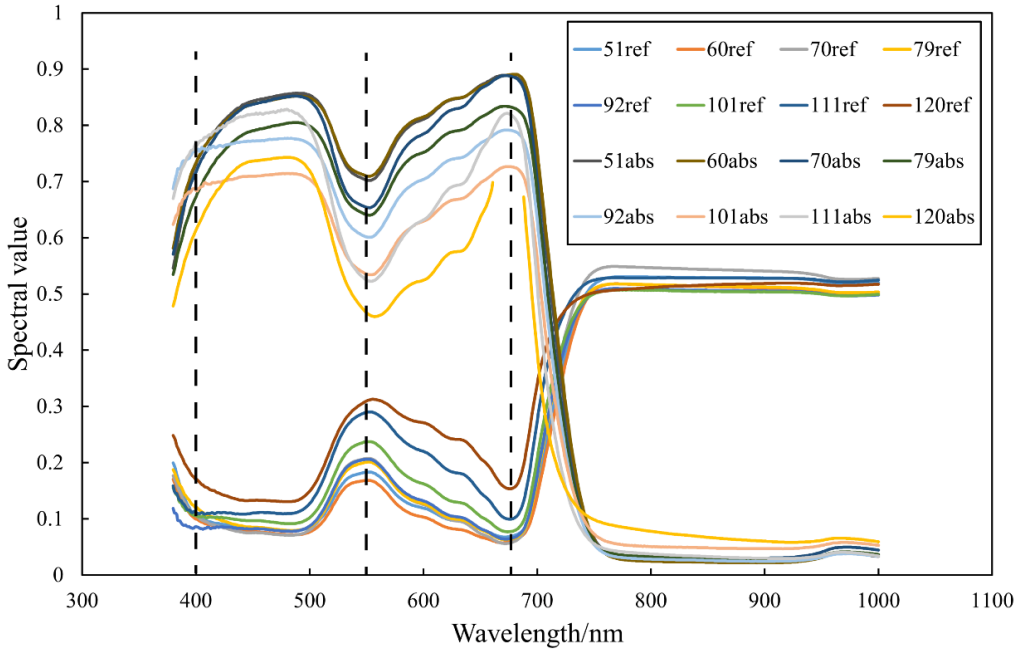

Figure 9. Temporal reflection spectra and absorption spectra of Zhong hua 11 under 1 N conditions (the number represents days after transplanting, ref represents reflectance spectra, and abs represents absorption spectra).

4.3. Comparative Analysis of Absorptivity and Reflectance in Inversion of Pigment Content

It can be seen from the results that, after the absorption spectrum of leaves is introduced, the vegetation index, based on the combination of the absorption spectrum and reflection spectrum, mostly improves the inversion accuracy of pigment content, which is confirmed in Figures 7 and 8. The pigment in plant leaves is mainly responsible for the absorption of light energy and the conversion of light energy into chemical energy, and so the level of pigment content and the absorption intensity of light are closely related. According to the propagation process of light in leaves, shown in Figure 2b, the light emitted by the light source illuminates the surface of the plant leaves. Then, part of the light is directly reflected by the epidermal cells of the leaves and is received by the instrument, part of the light is transmitted, and the light is reflected and transmitted again through the leaves and is received by the instrument. In this process, part of the light is absorbed by the blade, and part of the light is reflected by the blade, so the reflectivity detected by the instrument is partly from the direct reflection of the blade and partly from the reflection after transmission. According to the microstructure of plant leaves in Figure 2c, the epidermal cells of the leaves are convex upward. This is conducive to the accumulation of light in palisade parenchyma cells and the enhancement of light absorption in the leaves [63–65]. Both the light coming in from above and the light propagating upward after transmis-

sion are subject to the light-gathering effect in the bulges of the epidermal cells. At the same time, the sieve effect theory holds that light is heavily absorbed by strong absorbing molecules (such as chlorophyll, water, and other compounds, etc.) gathered in a small part of the cell volume (such as organelles) during the process of propagation inside the leaf, reducing the interaction and absorption opportunities of other molecules and light [61]. Evans et al. [66] showed that this phenomenon was most obvious at wavelengths where the light was strongly absorbed (blue and red bands). Based on this phenomenon, the vegetation index of the absorption spectrum was introduced in this study to improve the model's performance in pigment inversion, which verified the previous theory. Therefore, these characteristics of the leaves determine that the absorption spectrum of the leaves will transmit more information related to the pigment content, and so the correlation between the vegetation index and the pigment content is improved by introducing the absorption spectrum. Working based on the results, the absorption spectra of pigment absorption-sensitive bands (400 nm, 550 nm, 680 nm, and red-edge bands) were used to replace the relevant bands in the traditional vegetation index based on reflectance, and the inversion effect of pigment content was improved to a certain extent.

To sum up, the reflectance spectrum of the leaf cannot truly reflect the material content and structural characteristics of the leaf, while the absorption spectrum of the leaf accounts for the spectral characteristics presented by the photochemical reaction between light and the substances inside the leaf. The substances in the leaf that undergo the photochemical reaction are chlorophyll and carotenoids. Therefore, the vegetation index, used in combination with reflectance and absorptivity, is more effective than others in terms of inverting leaf pigment content.

5. Conclusions

According to the data collation and analysis performed in this experiment, the chlorophyll and carotenoid contents of different varieties of rice under different nitrogen fertilizer application rates showed an obvious change trend in the whole growth period, and the chlorophyll content showed a trend of first increasing and then decreasing with the growth period. However, the chlorophyll content of different varieties had different decreasing periods. The carotenoid content changed more obviously during the whole growth period, showing a gradually decreasing trend. In the process of using spectral data to invert the pigment content of leaves, it was found that using only the reflectance spectrum or absorptivity spectrum to invert the pigment content of leaves had certain defects. Replacing the reflectance of the traditional vegetation index with the form of combining reflectance and absorptivity, the new vegetation index showed a certain level of improvement in relation to the accuracy of retrieving pigment content. This study focused on the influence of the structural characteristics of leaf cells on light transmission in leaves, and so this idea can be extended to more types of plant leaves. The method in this study can be applied to upper epidermal mesophyll cells in leaves with a light-gathering effect. In the future, we will consider extending this research idea to the scale of vegetation canopy and inverting canopy pigment content based on the reflectivity and absorptivity of the canopy. We will consider the use of the canopy spectral invariant theory to calculate the corresponding canopy absorption, transmission, and reflection spectra using leaf reflection, absorption, and transmission spectra and related canopy structural parameters, and employ measurable spectra to test the accuracy of scale transformation. If this idea is feasible, it will further expand the application prospects of this research.

Author Contributions: L.M.: conceptualization, methodology, visualization, and writing the original draft. Y.L.: conceptualization and investigation. N.Y.: collecting the data. X.L.: collecting the data. Y.Y. collecting the data. C.Z.: collecting the data. S.F.: review and editing. Y.G.: conceptualization, review, and editing. All authors have read and agreed to the published version of the manuscript.

Funding: This research was funded by Ministry of Science and Technology of the People's Republic of China: Advance Research Project: Remote sensing inversion of key land surface elements and development of quantitative products.

Institutional Review Board Statement: Not applicable.

Data Availability Statement: Dataset available on request from the authors.

Acknowledgments: We thank the editor and reviewers for their constructive comments on this manuscript.

Conflicts of Interest: The authors declare that they have no known competing financial interests or personal relationships that could have appeared to influence the work reported in this paper.

References

1. Zeigler, R.S.; Barclay, A. *The Relevance of Rice*; Springer: Berlin/Heidelberg, Germany, 2008; pp. 3–10.
2. Zheng, J.; Song, X.; Yang, G.; Du, X.; Mei, X.; Yang, X. Remote sensing monitoring of rice and wheat canopy nitrogen: A review. *Remote Sens.* **2022**, *14*, 5712. [CrossRef]
3. Zheng, Q.; Huang, W.; Xia, Q.; Dong, Y.; Ye, H.; Jiang, H.; Chen, S.; Huang, S. Remote Sensing Monitoring of Rice Diseases and Pests from Different Data Sources: A Review. *Agronomy* **2023**, *13*, 1851. [CrossRef]
4. Spafford, L.; Le Maire, G.; MacDougall, A.; De Boissieu, F.; Féret, J.B. Spectral subdomains and prior estimation of leaf structure improves PROSPECT inversion on reflectance or transmittance alone. *Remote Sens. Environ.* **2021**, *252*, 112176. [CrossRef]
5. Frank, H.A.; Cogdell, R.J. Carotenoids in photosynthesis. *Photochem. Photobiol.* **1996**, *63*, 257–264. [CrossRef] [PubMed]
6. Ritz, T.; Damjanović, A.; Schulten, K.; Zhang, J.; Koyama, Y. Efficient light harvesting through carotenoids. *Photosynth. Res.* **2000**, *66*, 125–144. [CrossRef]
7. Hernández-Clemente, R.; Navarro-Cerrillo, R.M.; Suárez, L.; Morales, F.; Zarco-Tejada, P.J. Assessing structural effects on PRI for stress detection in conifer forests. *Remote Sens. Environ.* **2011**, *115*, 2360–2375. [CrossRef]
8. Kira, O.; Linker, R.; Gitelson, A. Non-destructive estimation of foliar chlorophyll and carotenoid contents: Focus on informative spectral bands. *Int. J. Appl. Earth Obs.* **2015**, *38*, 251–260. [CrossRef]
9. Wang, Z.; Chen, J.; Fan, Y.; Cheng, Y.; Wu, X.; Zhang, J.; Wang, B.; Wang, X.; Yong, T.; Liu, W. Evaluating photosynthetic pigment contents of maize using UVE-PLS based on continuous wavelet transform. *Comput. Electron. Agric.* **2020**, *169*, 105160. [CrossRef]
10. Beć, K.B.; Grabska, J.; Bonn, G.K.; Popp, M.; Huck, C.W. Principles and applications of vibrational spectroscopic imaging in plant science: A review. *Front. Plant Sci.* **2020**, *11*, 1226. [CrossRef]
11. Cavaco, A.M.; Utkin, A.B.; Marques Da Silva, J.; Guerra, R. Making Sense of Light: The Use of Optical Spectroscopy Techniques in Plant Sciences and Agriculture. *Appl. Sci.* **2022**, *12*, 997. [CrossRef]
12. Jang, I.T.; Lee, J.H.; Shin, E.J.; Nam, S.Y. Evaluation of Growth, Flowering, and Chlorophyll Fluorescence Responses of Viola cornuta cv. Penny Red Wing according to Spectral Power Distributions. *J. People Plants Environ.* **2023**, *26*, 335–349. [CrossRef]
13. Park, B.G.; Lee, J.H.; Shin, E.J.; Kim, E.A.; Nam, S.Y. Light quality influence on growth performance and physiological activity of Coleus cultivars. *Int. J. Plant Biol.* **2024**, *15*, 807–826. [CrossRef]
14. Zhao, R.; An, L.; Tang, W.; Qiao, L.; Wang, N.; Li, M.; Sun, H.; Liu, G. Improving chlorophyll content detection to suit maize dynamic growth effects by deep features of hyperspectral data. *Field Crops Res.* **2023**, *297*, 108929. [CrossRef]
15. Nagy, A.; Szabó, A.; Elbeltagi, A.; Nxumalo, G.S.; Bódi, E.B.; Tamás, J. Hyperspectral indices data fusion-based machine learning enhanced by MRMR algorithm for estimating maize chlorophyll content. *Front. Plant Sci.* **2024**, *15*, 1419316. [CrossRef] [PubMed]
16. Wang, T.; Gao, M.; Cao, C.; You, J.; Zhang, X.; Shen, L. Winter wheat chlorophyll content retrieval based on machine learning using in situ hyperspectral data. *Comput. Electron. Agric.* **2022**, *193*, 106728. [CrossRef]
17. Xu, X.; Li, Z.; Yang, X.; Yang, G.; Teng, C.; Zhu, H.; Liu, S. Predicting leaf chlorophyll content and its nonuniform vertical distribution of summer maize by using a radiation transfer model. *J. Appl. Remote Sens.* **2019**, *13*, 34505. [CrossRef]
18. Li, Y.; Lai, Y.; Zhang, J.; Song, Y.; Jiang, X.; Feng, X.; Yang, X.; Zhang, C. Review on remote sensing inversion methods of Chlorophyll a in Taihu Lake. In *IOP Conference Series: Earth and Environmental Science*; IOP Publishing: Bristol, UK, 2020; p. 12135.
19. Danner, M.; Berger, K.; Wocher, M.; Mauser, W.; Hank, T. Efficient RTM-based training of machine learning regression algorithms to quantify biophysical & biochemical traits of agricultural crops. *ISPRS J. Photogramm.* **2021**, *173*, 278–296.
20. Liang, S. Recent developments in estimating land surface biogeophysical variables from optical remote sensing. *Prog. Phys. Geogr.* **2007**, *31*, 501–516. [CrossRef]
21. Zhang, L.; Zhang, L.; Du, B. Deep learning for remote sensing data: A technical tutorial on the state of the art. *IEEE Geosci. Remote Sens. Mag.* **2016**, *4*, 22–40. [CrossRef]
22. Sagan, V.; Peterson, K.T.; Maimaitijiang, M.; Sidike, P.; Sloan, J.; Greeling, B.A.; Maalouf, S.; Adams, C. Monitoring inland water quality using remote sensing: Potential and limitations of spectral indices, bio-optical simulations, machine learning, and cloud computing. *Earth-Sci. Rev.* **2020**, *205*, 103187. [CrossRef]
23. Zhang, Y.; Hui, J.; Qin, Q.; Sun, Y.; Zhang, T.; Sun, H.; Li, M. Transfer-learning-based approach for leaf chlorophyll content estimation of winter wheat from hyperspectral data. *Remote Sens. Environ.* **2021**, *267*, 112724. [CrossRef]
24. Ali, A.M.; Darvishzadeh, R.; Skidmore, A.; Heurich, M.; Paganini, M.; Heiden, U.; Mücher, S. Evaluating prediction models for mapping canopy chlorophyll content across biomes. *Remote Sens.* **2020**, *12*, 1788. [CrossRef]

25. Chaabouni, S.; Kallel, A.; Houborg, R. Improving retrieval of crop biophysical properties in dryland areas using a multi-scale variational RTM inversion approach. *Int. J. Appl. Earth Obs.* **2021**, *94*, 102220. [CrossRef]
26. Sun, J.; Wang, L.; Shi, S.; Li, Z.; Yang, J.; Gong, W.; Wang, S.; Tagesson, T. Leaf pigment retrieval using the PROSAIL model: Influence of uncertainty in prior canopy-structure information. *Crop J.* **2022**, *10*, 1251–1263. [CrossRef]
27. Jiang, J.; Comar, A.; Burger, P.; Bancal, P.; Weiss, M.; Baret, F. Estimation of leaf traits from reflectance measurements: Comparison between methods based on vegetation indices and several versions of the PROSPECT model. *Plant Methods* **2018**, *14*, 1–16. [CrossRef]
28. Jiao, Z.; Zhang, A.; Sun, G.; Fu, H.; Yao, Y. Hyperspectral image based vegetation index (HSVI): A new vegetation index for urban ecological research. In Proceedings of the 2021 IEEE International Geoscience and Remote Sensing Symposium IGARSS, Brussels, Belgium, 11–16 July 2021; pp. 8249–8252.
29. Serrano, L. Effects of leaf structure on reflectance estimates of chlorophyll content. *Int. J. Remote Sens.* **2008**, *29*, 5265–5274. [CrossRef]
30. Croft, H.; Arabian, J.; Chen, J.M.; Shang, J.; Liu, J. Mapping within-field leaf chlorophyll content in agricultural crops for nitrogen management using Landsat-8 imagery. *Precis. Agric.* **2020**, *21*, 856–880. [CrossRef]
31. Gitelson, A.A.; Gritz, Y.; Merzlyak, M.N. Relationships between leaf chlorophyll content and spectral reflectance and algorithms for non-destructive chlorophyll assessment in higher plant leaves. *J. Plant Physiol.* **2003**, *160*, 271–282. [CrossRef]
32. Gitelson, A.A.; Keydan, G.P.; Merzlyak, M.N. Three-band model for noninvasive estimation of chlorophyll, carotenoids, and anthocyanin contents in higher plant leaves. *Geophys. Res. Lett.* **2006**, *33*. [CrossRef]
33. Liang, L.; Yang, M.; Zhang, L.; Lin, H.; Zhou, X. Chlorophyll content inversion with hyperspectral technology for wheat canopy based on support vector regression algorithm. *Trans. Chin. Soc. Agric. Eng.* **2012**, *28*, 162–171.
34. Qiao, L.; Gao, D.; Zhao, R.; Tang, W.; An, L.; Li, M.; Sun, H. Improving estimation of LAI dynamic by fusion of morphological and vegetation indices based on UAV imagery. *Comput. Electron. Agric.* **2022**, *192*, 106603. [CrossRef]
35. McClendon, J.H.; Fukshansky, L. On the interpretation of absorption spectra of leaves–I. Introduction and the correction of leaf spectra for surface reflection. *Photochem. Photobiol.* **1990**, *51*, 203–210. [CrossRef]
36. Baranoski, G.V.; Van Leeuwen, S.R. Detecting and monitoring water stress states in maize crops using spectral ratios obtained in the photosynthetic domain. *J. Appl. Remote Sens.* **2017**, *11*, 36025. [CrossRef]
37. Ustin, S.L.; Jacquemoud, S. How the optical properties of leaves modify the absorption and scattering of energy and enhance leaf functionality. In *Remote Sensing of Plant Biodiversity*; Spinger: Berlin/Heidelberg, Germany, 2020; pp. 349–384.
38. Eng, D.; Baranoski, G.V. The application of photoacoustic absorption spectral data to the modeling of leaf optical properties in the visible range. *IEEE Trans. Geosci. Remote* **2007**, *45*, 4077–4086. [CrossRef]
39. Dawson, T.P.; Curran, P.J.; Plummer, S.E. LIBERTY—Modeling the effects of leaf biochemical concentration on reflectance spectra. *Remote Sens. Environ.* **1998**, *65*, 50–60. [CrossRef]
40. Maier, S.W.; Lüdeker, W.; Günther, K.P. SLOP: A revised version of the stochastic model for leaf optical properties. *Remote Sens. Environ.* **1999**, *68*, 273–280. [CrossRef]
41. Jacquemoud, S.; Ustin, S.L. Modeling leaf optical properties. *Photobiol. Sci. Online* **2008**, *736*, 737.
42. Lichtenthaler, H.K.; Wellburn, A.R. *Determinations of Total Carotenoids and Chlorophylls a and b of Leaf Extracts in Different Solvents*; Portland Press Ltd.: London, UK, 1983.
43. Sims, D.A.; Gamon, J.A. Relationships between leaf pigment content and spectral reflectance across a wide range of species, leaf structures and developmental stages. *Remote Sens. Environ.* **2002**, *81*, 337–354. [CrossRef]
44. Terashima, I.; Saeki, T. Light environment within a leaf I. Optical properties of paradermal sections of Camellia leaves with special reference to differences in the optical properties of palisade and spongy tissues. *Plant Cell Physiol.* **1983**, *24*, 1493–1501. [CrossRef]
45. Vogelmann, T.C.; Bornman, J.F.; Yates, D.J. Focusing of light by leaf epidermal cells. *Physiol. Plant.* **1996**, *98*, 43–56. [CrossRef]
46. Datt, B.; McVicar, T.R.; Van Niel, T.G.; Jupp, D.L.; Pearlman, J.S. Preprocessing EO-1 Hyperion hyperspectral data to support the application of agricultural indexes. *IEEE Trans. Geosci. Remote Sens.* **2003**, *41*, 1246–1259. [CrossRef]
47. Gitelson, A.A.; Viña, A.; Ciganda, V.; Rundquist, D.C.; Arkebauer, T.J. Remote estimation of canopy chlorophyll content in crops. *Geophys. Res. Lett.* **2005**, *32*. [CrossRef]
48. Inoue, Y.; Peñuelas, J.; Miyata, A.; Mano, M. Normalized difference spectral indices for estimating photosynthetic efficiency and capacity at a canopy scale derived from hyperspectral and CO_2 flux measurements in rice. *Remote Sens. Environ.* **2008**, *112*, 156–172. [CrossRef]
49. Inoue, Y.; Sakaiya, E.; Zhu, Y.; Takahashi, W. Diagnostic mapping of canopy nitrogen content in rice based on hyperspectral measurements. *Remote Sens. Environ.* **2012**, *126*, 210–221. [CrossRef]
50. Jacquemoud, S.; Baret, F. PROSPECT: A model of leaf optical properties spectra. *Remote Sens. Environ.* **1990**, *34*, 75–91. [CrossRef]
51. Datt, B. Remote sensing of chlorophyll a, chlorophyll b, chlorophyll a+ b, and total carotenoid content in eucalyptus leaves. *Remote Sens. Environ.* **1998**, *66*, 111–121. [CrossRef]
52. Wang, S.; Zhu, Y.; Jiang, H.; Cao, W. Positional differences in nitrogen and sugar concentrations of upper leaves relate to plant N status in rice under different N rates. *Field Crops Res.* **2006**, *96*, 224–234. [CrossRef]
53. Gong, J.; Xing, Z.; Hu, Y.; Zhang, H.; Huo, Z.; Xu, K.; Wei, H.; Gao, H. Difference of characteristics of photosynthesis, matter production and translocation between indica and japonica super rice. *Acta Agron. Sin.* **2014**, *40*, 497–510. [CrossRef]

54. Dhami, N.; Cazzonelli, C.I. Environmental impacts on carotenoid metabolism in leaves. *Plant Growth Regul.* **2020**, *92*, 455–477. [CrossRef]
55. Bode, S.; Quentmeier, C.C.; Liao, P.; Hafi, N.; Barros, T.; Wilk, L.; Bittner, F.; Walla, P.J. On the regulation of photosynthesis by excitonic interactions between carotenoids and chlorophylls. *Proc. Natl. Acad. Sci. USA* **2009**, *106*, 12311–12316. [CrossRef]
56. Maslova, T.G.; Markovskaya, E.F.; Slemnev, N.N. Functions of carotenoids in leaves of higher plants. *Biol. Bull. Rev.* **2021**, *11*, 476–487. [CrossRef]
57. Nisar, N.; Li, L.; Lu, S.; Khin, N.C.; Pogson, B.J. Carotenoid metabolism in plants. *Mol. Plant* **2015**, *8*, 68–82. [CrossRef] [PubMed]
58. Rottet, S.; Devillers, J.; Glauser, G.; Douet, V.; Besagni, C.; Kessler, F. Identification of plastoglobules as a site of carotenoid cleavage. *Front. Plant Sci.* **2016**, *7*, 1855. [CrossRef] [PubMed]
59. Kume, A. Importance of the green color, absorption gradient, and spectral absorption of chloroplasts for the radiative energy balance of leaves. *J. Plant Res.* **2017**, *130*, 501–514. [CrossRef] [PubMed]
60. Moss, R.A.; Loomis, W.E. Absorption spectra of leaves. I. The visible spectrum. *Plant Physiol.* **1952**, *27*, 370. [CrossRef]
61. Cavender-Bares, J.; Gamon, J.A.; Townsend, P.A. *Remote Sensing of Plant Biodiversity*; Springer Nature: Berlin/Heidelberg, Germany, 2020.
62. Huang, S.; Tang, L.; Hupy, J.P.; Wang, Y.; Shao, G. A commentary review on the use of normalized difference vegetation index (NDVI) in the era of popular remote sensing. *J. For. Res.* **2021**, *32*, 1–6. [CrossRef]
63. Haberlandt, G. *Physiological Plant Anatomy*; Macmillan and Company, Limited: Ayrshire, Scotland, 1914.
64. Martin, G.; Josserand, S.A.; Bornman, J.F.; Vogelmann, T.C. Epidermal focussing and the light microenvironment within leaves of Medicago sativa. *Physiol. Plant.* **1989**, *76*, 485–492. [CrossRef]
65. Poulson, M.E.; Vogelmann, T.C. Epidermal focussing and effects upon photosynthetic light-harvesting in leaves of Oxalis. *Plant Cell Environ.* **1990**, *13*, 803–811. [CrossRef]
66. Evans, J.R.; Vogelmann, T.C.; Williams, W.E.; Gorton, H.L. Chloroplast to leaf. In *Photosynthetic Adaptation: Chloroplast to Landscape*; Springer: New York, NY, USA, 2004; pp. 15–41.